University of New Hampshire

University of New Hampshire Scholars' Repository

Spring 2022

Measuring the Ne/O Ratio for IMAP-Lo

Ryan J. Murphy
University of New Hampshire, Durham

Follow this and additional works at: https://scholars.unh.edu/honors

Determining the N/O Abundance Ratio for IMAP-Lo: Resolving the C/O Ratio for Ne using $1\mu g/cm^2$ Carbon Foils

Ryan Murphy[*]

University of New Hampshire, Durham, NH, 03824, USA

(Dated: May 24, 2022)

This paper aims to study if the thinner carbon foils of IMAP-Lo will lead to a better resolution of the C/O ratio and by extension, the Ne/O ratio. This is done by fitting an asymmetric kappa function to the time of flight spectra of both types of carbon foils. The ETU used in the most recent round of IMAP-Lo testing is outfitted with both $2\mu g/cm^2$ and $1\mu g/cm^2$ foils letting us create a model relating how the spectra change in response to different foil thickness. Using this model and validating it against test results, we simulate what we would expect to see from spectra of C and O generated from IBEX-Lo calibration data if they were to be measured using $1\mu g/cm^2$ foils that will be used in IMAP-Lo. This simulation shows that the energy straggling tails of the spectra are lessened when using the thinner foils.

I. INTRODUCTION

NASA's IMAP and IBEX missions both seek to answer the question of what exactly is happening at the edge of the solar system.[1] IBEX launched in 2008 and over the course of its lifetime has led to some fascinating science such as the discovery of the heliospheric ribbon.[2] Now IMAP is set to succeed IBEX and will hopefully give us even more insight into what the boundary between the heliosphere and the Interstellar Medium (ISM) is really like. Especially in light of the Astrophysics 2020 decadal, which lists one of the focuses of astrophysics in the next decade to be the study of exoplanets, understanding of our own solar system is crucial if we are to be looking for Earth-like planets outside it. Both IMAP and IBEX aim to gain this understanding by measuring Energetic Neutral Atoms (ENA) coming in from the boundary of the heliosphere as well as neutrals in the InterStellar Neutral (ISN) wind that flows into the solar system from the ISM. IMAP and IBEX are broken into multiple different instruments which measure different energy ranges of these neutral atoms. This paper will focus mainly on IMAP-Lo and IBEX-Lo which covers the energy regime of 10-1000 eV and 10-2000 eV, respectively.[3][4] Before we get to the matter at hand, it is important to first introduce the concepts and motivation that we are building on. To that end, the following sections will introduce the heliosphere, specifics of IMAP-Lo's subsections, and the carbon to oxygen (C/O) distribution in order to motivate the claim that IMAP-Lo having thinner carbon foils in it's time of flight subsystem should lead to better resolution for the Ne/O ratio of the ISM compared to IBEX-Lo.

The Ne/O ratio is of interest not just because they are both some of the most abundant elements in the galaxy, but also because there are multiple conflicting measurements of the interstellar Ne/O ratio. Juett et al. used X-ray spectroscopy on the absorption edges in X-ray binaries to find a Ne/O ratio of 0.185 ± 0.055.[5] This is in line with the solar abundance ratio and what we would expect to see. However, when Gloeckler and Fisk looked into the gas phase of the local ISM's pickup ion data, then found a Ne/O ratio of 0.38.[6] This is much higher than the solar value and suggests that a fraction of the ISM's gaseous oxygen is trapped somehow in some kind of dust or ice.[7] With the ratio being the key to determining just what is happening to the interstellar oxygen, it is important that we can resolve it to the best of our ability. IBEX-Lo's measurement of 0.4 ± 0.15 agreed with Fisk et al., but the relative error is large.[7] This is due to the error associated with calibrating Ne using the C/O ratio as will be discussed shortly. Reducing the uncertainty in this measurement is the motivation of this paper and why we are concerned with how measurements made with the new IMAP-Lo system will compare to those of IBEX-Lo.

This paper will introduce the heliosphere and interstellar medium before moving on to an overview of the IMAP-Lo instrument. In that overview we will discuss the different subsystems of IMAP-Lo and how they come together and interact to detect interstellar neutral atoms. Then we will identify why Ne is a problematic element

to measure and how we calibrate the instrument to be able to detect it. After introducing these concepts, we will move on the the analysis. With IBEX-Lo calibration data and IMAP-Lo ETU testing data, we will create a fitting routine for time of flight spectra and use it to create a model simulating how these spectra change in response to thinner carbon foils. This will let us simulate how the resolution of the C/O ratio might be changed when using IMAP-Lo.

II.   BASICS OF THE HELIOSPHERE

Our solar system, or the heliosphere, can be thought of as the volume carved out of our galactic neighborhood in the Milky Way by the sun's solar wind. The heliosphere acts as our shield from the interstellar cosmic rays that would bombard us otherwise. Moving away from the sun, the parts of the heliosphere are the termination shock, inner heliosheath, and outer heliosheath as shown in Fig. 1.[8] Much like how our sun emits solar wind outward, as we move through the Local Interstellar Cloud, the particles we move through flow towards us in what we call the interstellar wind. The heliopause, the boundary of the heliosphere, is created when the incoming pressure of this interstellar wind is balanced out by the outgoing pressure of the solar wind. This is through both ram and thermal pressure from the particles as well as the magnetic pressure from the fields carried by the plasma. However, as this boundary is created due to interactions between the stellar and interstellar plasmas, neutral gasses from the ISM are not stopped at the heliopause. Fig. 1 shows the path of this neutral interstellar wind. The neutrals that make it back to us are the ones that our instruments measure. IMAP-Lo and IBEX-Lo can even differentiate between different species of neutrals which is important for learning the species distribution of the ISM as that information can tell us a lot about the conditions outside of the solar system.

III.   OVERVIEW OF THE INSTRUMENT

IMAP-Lo and IBEX-Lo are neutral atom detectors able to measure and discern the species of neutral atoms through the use of Time Of Flight (TOF) mass spec-
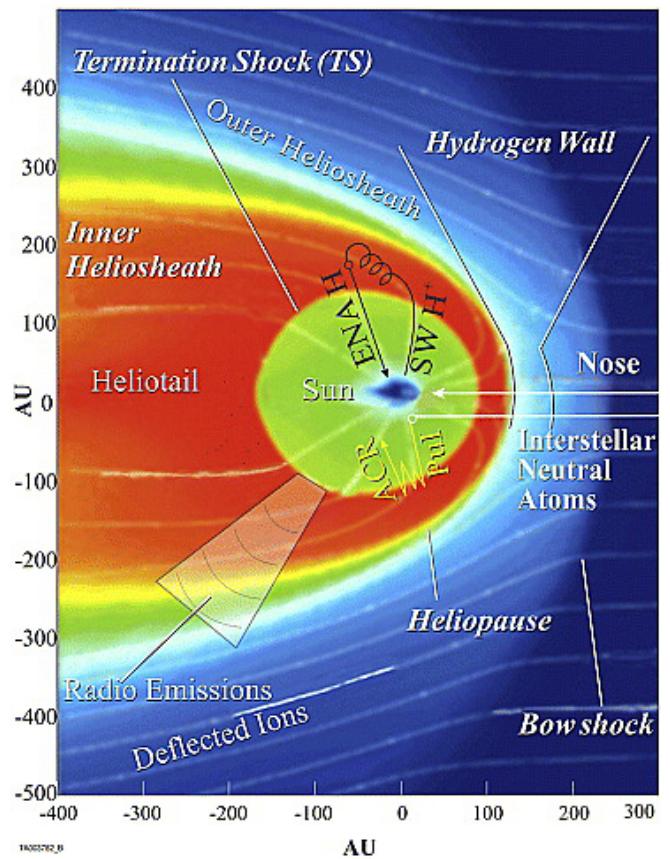

Figure 1. (From [9]) A model of the various parts of the heliosphere. In yellow is the edge of the termination shock leading into the inner and outer heliosheath. At the very edge of the heliosphere is the heliopause, which transitions directly into the interstellar medium here depicted in the blue colors indicating lower temperature. This figure also shows how the interstellar neutral wind flows towards the bow of the heliosphere.

troscopy. The first step of the detector is the entrance system, which collimates the incoming particles so that only those within a narrow field of view can enter the instrument. In order to suppress background readings, a pair of electrodes at 4keV are placed in front of the collimator to deflect incoming electrons with energy < 600 eV. Additionally, the entire collimator system floats at 3keV in order to keep out ions with energy < 3 keV.[3] The entrance system ensures that only neutral atoms, UV radiation, and very high energy ions make it into the instrument. The particles' next step when they enter the detector is to make contact with a diamond-like carbon conversion surface which converts a portion of the particles into negatively charged ions (see Fig. 2. This col-
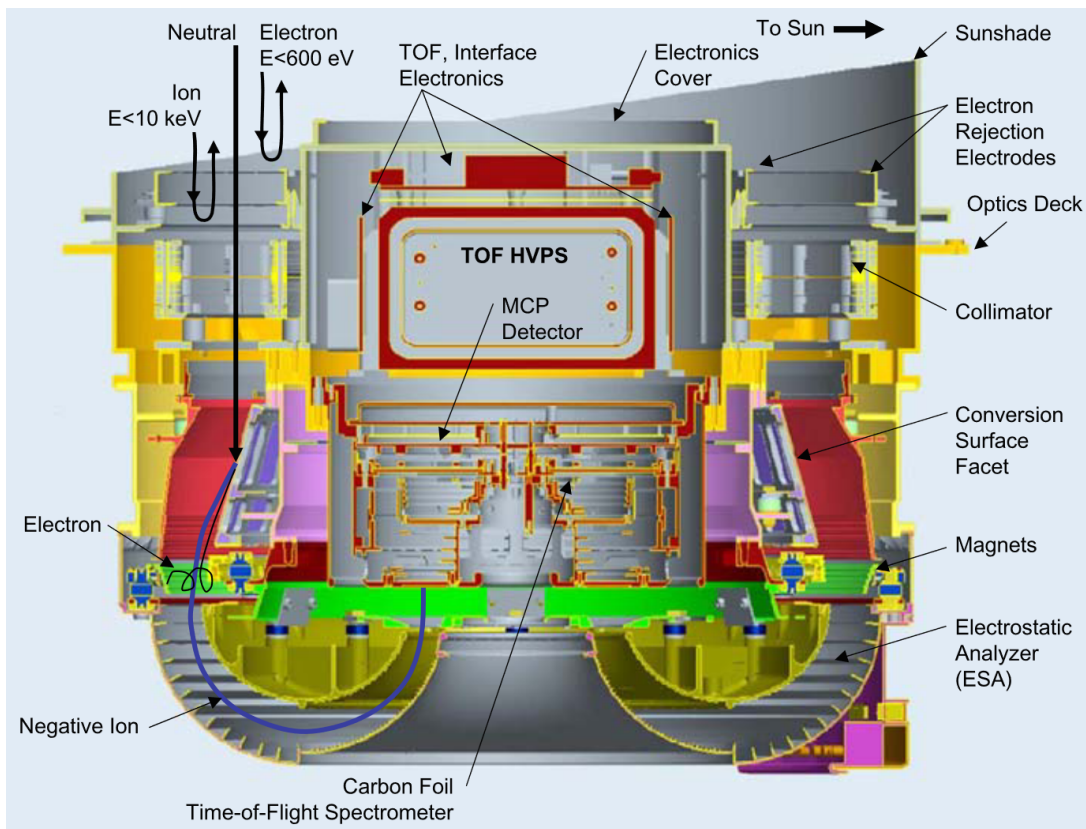
Figure 2. (From [4]) A cross section of the IBEX-Lo instrument. Aside from the sunshade, the instrument is rotationally symmetric. IMAP-Lo is mostly identical except for the voltages and placement of the electrodes within the entrance subsystem. The black lines indicate the particles trajectories. The particles are collimated and selected by the entrance before a fraction of them are ionized and deflected upon collision with the conversion surface. After making contact with the conversion surface, the ions are accelerated into the electrostatic analyzer. The ESA filters the particles, only allowing those of a certain energy band to pass into the time of flight subsection.

lision with the conversion surface also creates sputtered byproducts of H, C, and O.[7] This is vital for certain elements, such as Ne, which cannot be directly converted to a stable negative ion. This will be discussed more in section 4. After being deflected off of the conversion surface, the ions are accelerated through a ring of magnets that separate secondary and photo-electrons before passing into the ElectroStatic Analyzer (ESA).[3]

The ESA has two important purposes within the instrument. Firstly, the inner and outer electrodes create an electric field that pulls the negative ions along the curved path (see Fig. 2). This electric field only allows ions of a certain energy range to pass through. Ions with not enough energy will be deflected by the electric field into the walls of the ESA before making it through the curve and ions with too much energy will not be deflected enough. If we vary the voltage across the electrodes, we

can change this energy range and selectively look at particles in a certain energy band. The second purpose is to stop the previously mentioned UV radiation from getting any further in the instrument. The walls of the ESA are blackened with an Au black surface which, in tandem with the curved structure, will ensure that no UV radiation makes it to the actual detector and overloads the readings.

Now onto the TOF proper. As the particles exit the ESA, they enter a high voltage region called the Post ACceleration (PAC). Again, for reference, IMAP-Lo's ESA can analyze particles in the range of 10-1000 eV, although that top end is rarely reached. The voltage across the PAC is 16keV which is much higher than the initial energy of the particles. This ensures that the particles have enough energy to pierce through the carbon foils thereby reducing energy loss of the particles inside the TOF. Af-
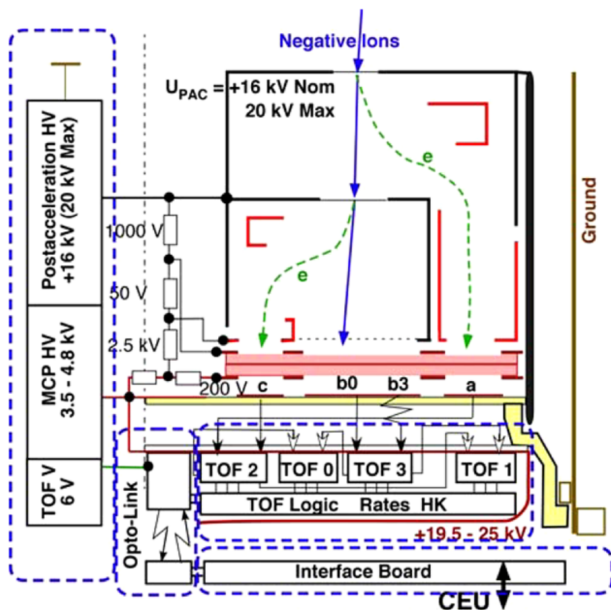
Figure 3. (From [4]) Cross section of the Time of Flight subsection for IBEX-Lo. For IMAP,the difference is in the thickness of the carbon foils. The ion trajectories are shown in blue coming out of the post acceleration from the top of the figure. The ions pass through carbon foils of thickness $1\mu/cm^2$ and $2\mu g/cm^2$ for IMAP-Lo and IBEX-Lo respectively. The collision with the first foil knocks off the first set of secondary electrons (shown in green) which are deflected and accelerated into the multichannel plate (shown in red), creating the start pulse. The ions continue, colliding again with the second foil and knocking off more electrons. This creates the second start signal. The ions themselves then hit the MCP where they trigger the stop pulse.

ter being accelerated through the PAC, the true TOF mass spectroscopy begins. After leaving the PAC, the ions are in the TOF subsection. The TOF is a triple coincidence mass spectrometer with a known distance that the particles must travel through, and since their energy is mostly defined by the PAC, we can resolve the mass of the individual particles , and therefore their species, with some simple kinetic energy calculations.

$$T = \frac{1}{2}mv^2 \tag{1}$$

Where T is the energy of the particles leaving the PAC. Since the initial energy of the particle is small compared to the energy gained going through the PAC, it is a reasonable assumption to set the energy of the particles to the energy of the PAC for these TOF calculations. Since

we now know the energy of the incoming particles, if we can determine their velocity then we can also infer their mass. The distance across the TOF is known so, by measuring the time it takes for the particle to travel through, we can solve for v using $v = d/t$. This time the particles take to travel across the TOF is measured through the use of two carbon foils and a MicroChannel Plate (MCP). When the negative ions collide with the foils, secondary electrons will be knocked off, deflected, and accelerated down the TOF to be detected by start/stop electrodes on the MCP (see Fig. 3). The MCP will have three readings from the collisions per particle. Two from the secondary electrons, and one from the particle itself. The distance between the first and second foils is called TOF2, the distance between the second foil and the MCP is called TOF1, and the total distance is called TOF0. There is also a TOF3 which is the delay time between the different sections of the MCP. The reason for the triple coincidence is because the number of incoming neutral flux is very weak compared to background ions. Thus the coincidence of three signals is necessary to differentiate the signal from the background.[10] By using these TOF measurements and Eq. 1, we can infer the mass of the neutrals that we measure.

IV. NE AND THE CARBON TO OXYGEN RATIO

IMAP-Lo measures neutrals in the interstellar wind. Some of the most predominant elements in this wind are H, He, O, and Ne due to their high ionization energies leading to large neutral populations in the inner heliosphere. Said neutrals can be measured by IMAP-Lo using the process described in section 3, but there is a complication with elements such as Ne and He. These elements do not possess a stable negative ion and, therefore, cannot be properly converted by the conversion surface and filtered through the ESA in the same way that other elements can. Thankfully, there exists a way to measure them regardless. When a particle hits the conversion surface, C as well as H and O from the water film will be ionized and sputtered off due to the collision. The amount of these sputtered products is characteristic of the mass and energy of incident particle and can

be read in the same way as normal neutrals that were ionized by the conversion surface. If we fire a beam of Ne at the sensor, we will see a characteristic spectra of sputtered products that can be used as a calibration for the C/O ratio of Ne. Measuring this C/O gives us a way to measure when IMAP-Lo is measuring Ne. In other words, resolving the C/O ratio is the key that leads to measuring the Ne/O ratio.

Measuring the Ne/O ratio leads us to the heart of this paper. C and O have relatively similar times of flight due to being close in mass. The time of flight spectra are also not delta functions; they have a spread to them especially towards longer times of flight. This is due to the carbon foils in the TOF that knock off the secondary electrons. Colliding with the foils causes the particles to lose energy and extends their time of flight. Because of this, the peaks for each species have tails to their distributions from the energy straggling. This is especially problematic because the tail of the C peak bleeds over counts into the O peak, artificially inflating it. These uncertainties in measuring the C/O ratio make the resolution of measured Ne poor, as it is directly linked. For IBEX-Lo, there was a large relative error on the Ne/O ratio of 37.5% for ISN gas.[7] In order to lower this uncertainty, we need better resolution on our C to O ratio for the sputtering calibration. With a better resolution, Ne will be easier to measure and IMAP-Lo is outfitted with $1\mu g/cm^2$ carbon foils as opposed to the doubly thick $2\mu g/cm^2$ foils of IBEX-Lo. This will reduce the energy loss through the foils which will in turn lessen the effect of the energy straggling tail on the TOF spectra.[11] This paper aims to show that with the thinner foils of IMAP-Lo, the calibration of the C/O ratio will have better resolution leading to less uncertainty in the N/O ratio compared to IBEX-Lo, therefore ensuring that IMAP-Lo will provide us with more accurate data for the science objectives outlined for the project.

V. DATA ACQUISITION

This study uses data taken from the IBEX-Lo calibration done at the MEFISTO facility in the University of Bern. These calibrations consisted of firing neutral beams of single species (H, He, O , C, Ne) at the in-

strument where they can be read following the process outlined in section 3. We particularly care about the spectra of pure C and O as these kinds of spectra do not yet exist for IMAP-Lo. In order to test the fitting routine that will be discussed in section 6, we must have base spectra to work with so that we can see how well we are able to resolve the C/O ratio from flight data.

Data from IMAP-Lo was taken using the IMAP-Lo ETU and UNH ion beam facility. The IMAP-Lo ETU is outfitted with both $1\mu g/cm^2$ as is planned to be used on IMAP-Lo, and $2\mu g/cm^2$ in order to compare data between the foils. The ion beam was used to fire a beam of ionized gas consisting of H+, He+, O+, Ne+, and Ar+ at the instrument. Because this testing was performed on the TOF section of the ETU and not the full instrument, the conversion surface subsection was not involved in testing and therefore, the sputtering of Ne was not measurable. Not having the conversion surface was not a problem for generating TOF spectra as the particles were already ionized, however. As such, the TOF section ETU testing was able to create spectra of the constituent elements for both $1\mu g/cm^2$ and $2\mu g/cm^2$ foils.

Without MEFISTO data for IMAP-Lo, it is difficult to draw a direct comparison to the calibrations done with IBEX-Lo. However, with the pure spectra for C and O from IBEX-Lo, we can create a fitting routine and use it to decompose flight data as well as to analyze the ETU testing of IMAP-Lo. Since the ETU used for IMAP-Lo testing has data for both types of foils, if we can understand how the fits for the TOF spectra change with foils thickness, we can predict how the $2\mu g/cm^2$ C and O spectra of IBEX-Lo might change with thinner foils.

VI. ANALYSIS

A. Testing the Asymmetric Kappa Function

The first step to being able to resolve the C/O ratio from flight data is to have an appropriate fitting routine. We will use an asymmetric kappa function of the form,

$$N(t,\kappa) = \frac{A}{((t-t_0)^2\beta + 1)^{\kappa+1}}, \qquad (2)$$

where

$$\kappa = \frac{1}{2}(\kappa_r + \kappa_l) + \frac{1}{2}\frac{t-t_0}{|t-t_0|}(\kappa_r - \kappa_l). \qquad (3)$$
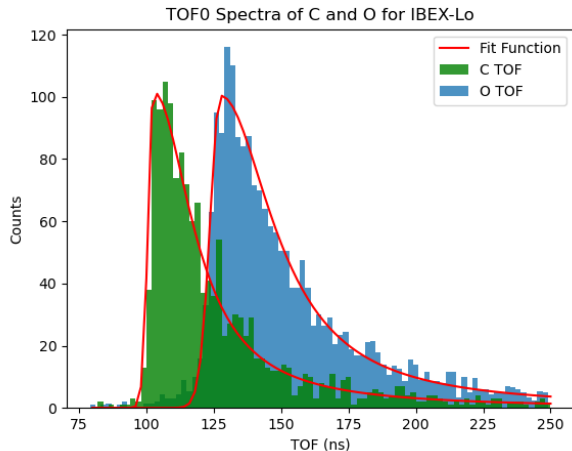
Figure 4. Individual TOF spectra for C and O taken from IBEX-Lo calibration data at the MEFISTO facility. These spectra were taken using energy step 8 for the ESA. This functions as the control for fitting flight data as well as the data for pure C and O using $2\mu g/cm^2$ carbon foils.
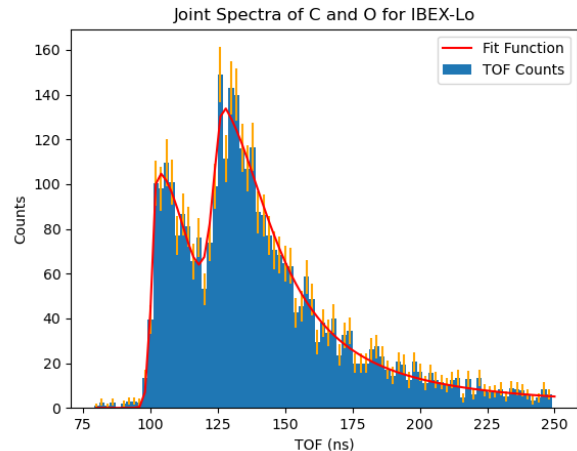

Figure 5. By adding the TOF spectra of C and O together, we can see what a real spectra with both elements present would look like. Using the individual fitting functions as a base, this fitting regime aims to extract the abundance ratio from concatenated TOF spectra. The orange error bars show the uncertainty in counts.

A and t_0 represents the height of the peak and the time it occurs. β is a measure of the inverse of the thickness of the distribution, σ and is defined by

$$\beta = \frac{1}{2\sigma}. \tag{4}$$

Finally, κ_r and κ_l define how each side of the function evolves. Due to the $t-t_0$ terms inside Eq (3), the function behaves differently to the left and right of t_0. Thus, it is an asymmetric kappa function.

We can see how this function looks in Fig. 4. This figure shows the pure spectra of C and O from the IBEX-Lo calibration overlaid on the same graph. Both TOF spectra have been fitted with the kappa function and one can see how the asymmetric nature of the fit comes into play. The right side falls off more slowly, capturing the behavior of the low energy tail and energy straggling through the carbon foils.

However, real flight data will not look like Fig. 4. The region of overlap between the spectra of C and O will be indistinguishable. Thus, the tail of C will "bleed over" into the O spectra and artificially inflate the counts. We can easily see this by adding the two spectra together and creating a more realistic sample of data. Fig. 5 shows what this new spectra would look like. We can see that the O peak which used to be at roughly the same amount of counts as C has been increased well above what it was

initially. In order to retrieve the original amount of C and O we can decompose the spectra using a linear combination of asymmetric kappa functions. By adding them together and fitting the flight data to the combination, each individual function will contain the decomposed fit of the individual element. Since we already have the pure spectra for C and O fit, we can use the parameters for those fits and set them as controls. If we force $t_0, \beta, \kappa_r,$ and κ_l to be the same as the pure fit, then all we need to solve for is A. A is a factor that controls the peak height and more broadly is a measure of the abundance. Therefore, with all other parameters fixed, solving for A lets us determine the abundance of the element being fit.

By integrating under the kappa distributions, we can find the total number of counts over a certain time frame. If we then divide the number of C counts by the number of O counts, we can determine the C/O ratio. The C/O ratio for the pure spectra as well as for the joint spectra are shown in Table I. These ratios are very close indicating that the joint fitting regime is capable of properly capturing the form of the spectra and extracting the original amount of C and O out of flight data. This is further supported by the reduced χ^2 of the fit being so close to 1. With this established, we can move forward confident in our fitting regime.

Fit	C/O	χ^2
Pure	0.74 ± 0.25	–
Joint	0.77 ± 0.26	0.89

Table I. The carbon to oxygen ratio taken by dividing the total number of counts of C by that of O.

B. Modeling Change in TOF Spectra Due to Thinner Carbon Foils

With calibration data for C and O and a fitting function capable of properly capturing the structure of TOF spectra in hand, it is time to put them to use. These tools will let us analyze the most recent tests in the UNH ion beam facility using the IMAP-Lo ETU and see the effect of our foils on the TOF measurements. The species characterization tests performed using the ETU were divided into heavy and light ions. Since we care about C and O, the heavy ion runs are what we want to analyze. Fig.6 shows spectra generated for TOF0 during said runs. Based on the locations of the peaks, the large peaks shown are likely Ne and Ar. It seems like there could be an small oxygen peak just before the Ne peak but it is buried within the Ne counts and would be difficult to decompose. As mentioned in Section V, the gas used in the ETU testing does not contain C so we cannot measure that peak either.

If we do not have spectra for C and O, then we will have to create a model to show how we expect them to evolve as a function of foil thickness. To create this model, we will make use of the Ne peak we see in Fig.6. Ne is just as close in mass to O as C is, so it is a reasonable assumption to say that the change in Ne's TOF spectra due to thinner foils would be emulated by C and O. Using the asymmetric kappa function, we create two fits for Ne. These are not precise fits of pure Ne as the onset of this peak is likely being inflated by O counts. Additionally, the rising flank of the Ar peak may be distorting the shapes of the Ne peaks. However, despite these two concerns, the fits are good enough for use in constructing the model. The last subplot of Fig. 6 shows the fit functions overlaid. The peaks are in different locations but we can see that the tail of the $1\mu g/cm^2$ spectra seems to fall off more sharply then that of the $2\mu g/cm^2$ spectra.

The fit parameters we are considering for the model are

$\kappa_l, \kappa_r, \beta$. Optimally, t_0 would be included as well as energy loss through foils also pushes t_0 to slower times.[11] However, in our ETU test data, we see that t_0 is actually higher for the $1\mu g/cm^2$ foils. This is contrary to our expectations. It is possible that the counts of the oxygen peak in the $2\mu g/cm^2$ spectra are causing t_0 to appear earlier than it would otherwise. Due to these uncertainties in whether the value of t_0 is accurate for the spectra, it has been excluded as a parameter in the model. For the other parameters we assume that the ratio between them between $2\mu g/cm^2$ and $1\mu g/cm^2$ is similar for Ne, C, and O. In other words, for a parameter "a",

$$\frac{a_{\text{Ne},1\mu g}}{a_{\text{Ne},2\mu g}} = \frac{a_{\text{O},1\mu g}}{a_{\text{O},2\mu g}} = \frac{a_{\text{C},1\mu g}}{a_{\text{C},2\mu g}}. \tag{5}$$
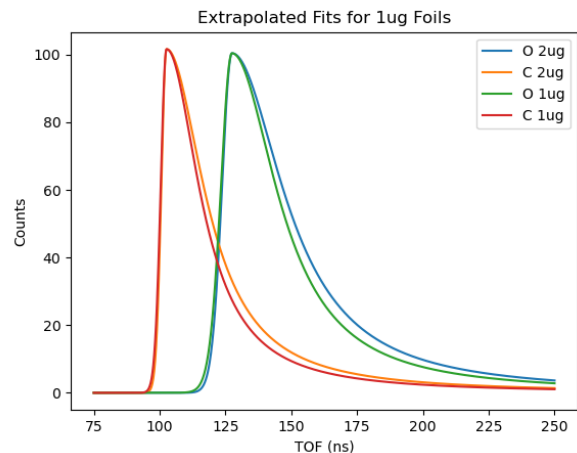

Figure 7. Fits of the $2\mu g/cm^2$ IBEX-Lo calibration data from MEFISTO as well as how those fits would be expected to look using the model. The energy straggling tails seem to be pulled in meaning that we can better seperate the C and O spectra.

Applying this assumption to the fit parameters of C and O using $2\mu g/cm^2$ foils from IBEX that we generated previously (see Fig. 4) produces the graphs shown in Fig. 7. The parameters used in creating these graphs are shown in Table II. As with the Ne peaks, we can see that the high energy tails of C and O are pulled in. This means that less counts of C and O are bleeding over into the spectra of the other and we can better separate the spectra and get a more resolved C/O ratio. The parameters used in creating these graphs are shown in Table II. We can see that both kappas decrease as a function of foil thickness as we would expect from simulations. β
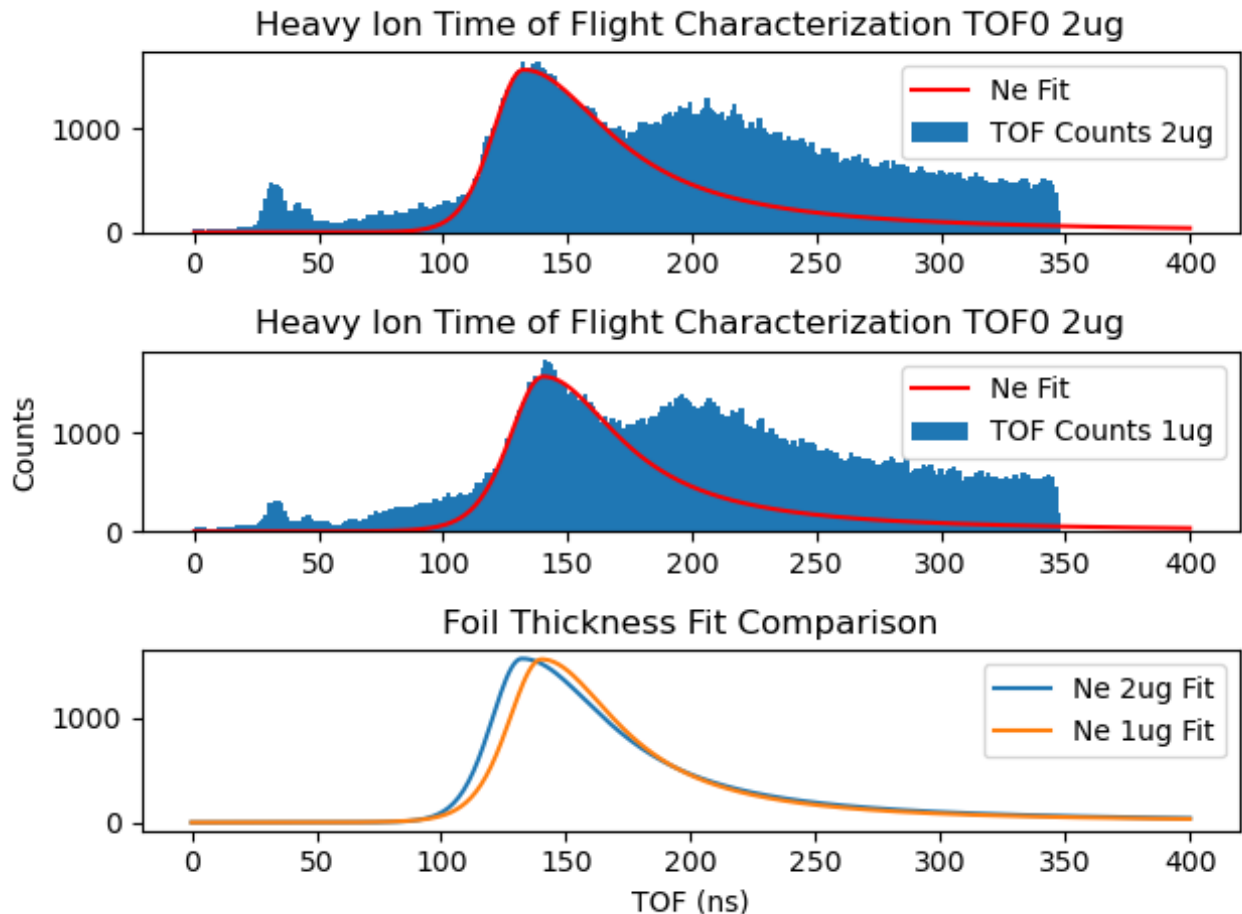
Figure 6. Spectra for both foil thicknesses from the heavy ion characterization tests using the IMAP-Lo TOF ETU. We fit the Ne peak in both and overlaid the functions in the bottom graph to show a direct comparison.

increases with the thinner foils, but one must remember from Eq (4) that β is an inverse to width of the distribution meaning that it being higher indicates a lower width.

VII. CONCLUSION

IMAP-Lo will be instrumental in answering many of the questions that IBEX-Lo created. In this paper, we discussed how we can use asymmetric kappa functions to fit and decompose the TOF spectra of flight data into its constituent elements. Using this fit function, we then used it to create a model of how our TOF spectra will change with $1\mu g/cm^2$ foils. We accomplished this by fitting Ne in recent heavy ion characterization data from the IMAP-Lo ETU and extrapolated that result to C and

O. We saw that the thinner foils should indeed reduce the energy straggling and taper in the high energy tails of C and O. This means that IMAP-Lo should have better seperation of C and O spectra leading to better resolution in the C/O ratio of Ne and, by extension, the Ne/O ratio in the ISM. Hopefully in the future this model will be corroborated by future IMAP-Lo testing.

VIII. ACKNOWLEDGEMENTS

I'd like to give a big thanks to all the members of the IMAP team. It has been a pleasure to work with all of you. Special thanks goes to my advisors Dr. Nathan Schwadron and Dr. Eberhard Moebius for their expertise and assistance throughout this whole process. Thanks are also due to Aly Aly for teaching me about the work-

Fit	κ_L	κ_R	β
Ne $2\mu g$	5.46 ± 8.89	$6.85E-16 \pm 1.02$	$5.26E-4 \pm 6.8E-4$
Ne $1\mu g$	3.30 ± 5.57	$1.06E-17 \pm 1.21$	$6.88E-4 \pm 9.86E-4$
O $2\mu g$	19.2 ± 5.90	$5.07E-23 \pm 9.21E-2$	$1.77E-3 \pm 3.21E-4$
O $1\mu g$	11.6 ± 27.5	$7.87E-25 \pm 3.43E-2$	$2.31E-3 \pm 4.43E-3$
C $2\mu g$	38.1 ± 14.3	$6.79E-23 \pm 9.29E-2$	$3.34E-3 \pm 6.85E-4$
C $1\mu g$	23.0 ± 54.7	$1.06E-24 \pm 3.45E-2$	$4.38E-3 \pm 8.50E-3$

Table II. By fitting the data for Ne using both foil thicknesses, we can see how the fit parameters evolve. By assuming that C and O behave similar to Ne since they are close in mass, the fit parameters of the MEFISTO fits can be modified to simulate similar tests being done with the thinner foils. Uncertainties in fit values were derived from scipy.optimize. These uncertainties were then propogated to find the uncertainties in the $1\mu g/cm^2$ C and O parameters.

ings of the asymmetric kappa function. A final mention goes to Jon Bower for being a mentor for me when I was first starting out with IMAP and for all the work he and the Morse 145 team have put into the lab.

* Corresponding author: rjm1068@usnh.edu

[1] D. J. McComas, F. Allegrini, P. Bochsler, M. Bzowski, M. Collier, H. Fahr, H. Fichtner, P. Frisch, H. O. Funsten, S. A. Fuselier, G. Gloeckler, M. Gruntman, V. Izmodenov, P. Knappenberger, M. Lee, S. Livi, D. Mitchell, E. Möbius, T. Moore, S. Pope, D. Reisenfeld, E. Roelof, J. Scherrer, N. Schwadron, R. Tyler, M. Wieser, M. Witte, P. Wurz, and G. Zank, **146**, 11 (2009).

[2] D. J. McComas, F. Allegrini, P. Bochsler, M. Bzowski, E. R. Christian, G. B. Crew, R. DeMajistre, H. Fahr, H. Fichtner, P. C. Frisch, H. O. Funsten, S. A. Fuselier, G. Gloeckler, M. Gruntman, J. Heerikhuisen, V. Izmodenov, P. Janzen, P. Knappenberger, S. Krimigis, H. Kucharek, M. Lee, G. Livadiotis, S. Livi, R. J. MacDowall, D. Mitchell, E. Möbius, T. Moore, N. V. Pogorelov, D. Reisenfeld, E. Roelof, L. Saul, N. A. Schwadron, P. W. Valek, R. Vanderspek, P. Wurz, and G. P. Zank, Science **326**, 959 (2009).

[3] D. J. McComas, E. R. Christian, N. A. Schwadron, N. Fox, J. Westlake, F. Allegrini, D. N. Baker, D. Biesecker, M. Bzowski, G. Clark, and et al., Space Science Reviews **214**, 10.1007/s11214-018-0550-1 (2018).

[4] S. A. Fuselier, P. Bochsler, D. Chornay, G. Clark, G. B. Crew, G. Dunn, S. Ellis, T. Friedmann, H. O. Funsten, A. G. Ghielmetti, and et al., Space Science Reviews **146**, 117–147 (2009).

[5] A. M. Juett, N. S. Schulz, D. Chakrabarty, and T. W. Gorczyca, Astrophys. J. **648**, 1066 (2006), arXiv:astro-ph/0605674 [astro-ph].

[6] G. Gloeckler and L. A. Fisk, **130**, 489 (2007).

[7] P. Bochsler, L. Petersen, E. Möbius, N. A. Schwadron, P. Wurz, J. A. Scheer, S. A. Fuselier, D. J. McComas, M. Bzowski, P. C. Frisch, and et al., The Astrophysical Journal Supplement Series **198**, 13 (2012).

[8] M.-B. Kallenrode, *Space physics: An introduction to plasmas and particles in the heliosphere and magnetospheres* (Springer, 2011).

[9] D. J. McComas, H. O. Funsten, S. A. Fuselier, W. S. Lewis, E. Möbius, and N. A. Schwadron, Geophysical Research Letters **38**, 10.1029/2011gl048763 (2011).

[10] E. Möbius, A. B. Galvin, L. M. Kistler, H. Kucharek, and M. A. Popecki, Journal of Geophysical Research: Space Physics **121**, 10.1002/2016ja022553 (2016).

[11] F. Allegrini, R. W. Ebert, G. Nicolaou, and G. Grubbs, Nuclear Instruments and Methods in Physics Research Section B: Beam Interactions with Materials and Atoms **359**, 115–119 (2015).